Screening of particle exchange in quantum Boltzmann liquids

K. A. Gernoth,[1] T. Lindenau,[2] and M. L. Ristig[2]
[1]*School of Physics and Astronomy, The University of Manchester, Manchester M13 9PL, United Kingdom*
[2]*Institut für Theoretische Physik, Universität zu Köln, D-50937 Köln, Germany*
(Received 23 July 2006; revised manuscript received 26 February 2007; published 14 May 2007)

We employ correlated density-matrix theory of strongly correlated Bose fluids to analyze the structural properties of quantum Boltzmann liquids. The constituents of such a normal quantum system are distinguishable as in a classical fluid since the interparticle forces prevent any exchange of identical bosons at short relative distances. Our study focuses on this particle-screening effect and on its consequences for the properties of various correlation functions, structure functions, momentum distributions, and quasiparticle and collective excitations. The formalism of the adopted microscopic theory is applied to a detailed numerical investigation of particle-screening properties and the quantum behavior of liquid para-hydrogen close to the triple point temperature. The theoretical results are compared with numerical data of path-integral Monte Carlo simulations and with available experimental results of recent cross-section measurements by neutron scattering.

DOI: 10.1103/PhysRevB.75.174204 PACS number(s): 61.20.Ja, 67.20.+k, 05.30.Jp

I. INTRODUCTION

The structure of correlated quantum fluids is determined by the effects of dynamical correlations, particle exchange, and interparticle phase correlations. Theoretical information on these correlations and other equilibrium properties of interest is stored in the N-body density matrix that completely describes the thermodynamic state of the fluid. Correlated density-matrix (CDM) theory[1,2] is a powerful and efficient tool to extract such information from the associated one-body and two-body reduced density-matrix elements and the corresponding Fourier transforms.

CDM theory is, in spirit, nonperturbative and therefore able to deal with quantum correlations of arbitrary strengths. At zero temperature, the CDM approach specializes to the correlated basis-functions theory[3,4] that has been very successfully applied to analyze correlated ground states of quantum liquids such as liquid helium[5] and quantum spin lattices.[6]

In the present study, we perform a CDM analysis of a special class of strongly correlated normal Bose fluids that may be called quantum Boltzmann liquids. A prototype of such a system is liquid *para*-hydrogen close to the triple point temperature. At appropriate temperatures and particle densities, the strongly repulsive interactions existing at short relative distances between and among the constituents are capable of screening their exchange. As a consequence, the particles of such a system remain distinguishable as they are at high temperatures in the classical thermodynamic regime, although the liquid exhibits significant quantum-mechanical effects.

Moving the correlated Bose system closer to the normal-phase boundary, the screening of particle exchange becomes incomplete and the particles no longer follow the classical exchange behavior. Finally, at the Bose-Einstein transition line, the bosonic exchange correlations develop long-range order in coordinate space and the particles are completely indistinguishable.

CDM theory of the normal phase of a boson fluid is built on a systematic construction of the associated Helmholtz free energy F as a functional of the static liquid structure function $S(k)$, the quasiparticle momentum distribution $n_{\mathrm{qp}}(k)$, and the occupation-number density $n_{\mathrm{coll}}(k)$ of the collective excitations. These functions are subsequently optimized by exploiting a minimum principle for the thermodynamic potential F. They may be calculated as solutions of three corresponding Euler-Lagrange equations. The optimal functions $S(k)$, $n_{\mathrm{qp}}(k)$, and $n_{\mathrm{coll}}(k)$ may then serve as input quantities to calculate associated functions of interest such as the radial distribution function $g(r)$, the one-body reduced density-matrix elements, excitation energies, etc. The development of this CDM formalism has been reported in Refs. 1 and 2.

We employ and specialize the CDM theory for a formal analysis of the structure and excitations of quantum Boltzmann liquids. The formalism is then applied to a numerical study of the properties of liquid *para*-hydrogen. We concentrate on the calculation of the radial distribution function $g(r)$, the structure function $S(k)$, the exchange correlation functions, and, in particular, the cyclic exchange structure function $S_{\mathrm{cc}}(k)$ at a temperature $T=16.5$ K and at three different particle-number densities corresponding to experimental pressures of 1, 40, and 80 bar. We extend the numerical analysis by calculating the collective excitation energy, the quasiparticle energy, and the momentum distribution as functions of wave number k. A detailed numerical analysis is presented on the one-body reduced density matrix $n(r)$, the corresponding momentum distribution $n(k)$ of a hydrogen molecule in the liquid, and the phase-phase correlation function $P(r)$.

The numerical study confirms that liquid *para*-hydrogen close to the triple point temperature is a typical quantum Boltzmann liquid. We demonstrate this property by a comparison between the numerical results derived within CDM theory (i) *without* any assumptions on possible screening effects and (ii) assuming complete screening of particle exchange from the *outset*. We further demonstrate the existence of significant quantum effects in the hydrogen liquid. The total kinetic energy is much larger than classical theory predicts. This well-known property is caused by the presence of strong phase-phase correlations in the liquid induced by the

 ©2007 The American Physical Society

particle-particle interactions. Moreover, there are distinct deviations of the kinetic-energy distribution in momentum space from the classical Maxwell distribution.[7] These theoretical results are compared with experimental results of recent measurements of neutron-scattering cross sections.[8] To check the accuracy of the CDM results on the radial distribution function $g(r)$ of liquid *para*-hydrogen, we have also performed path-integral Monte Carlo (PIMC) simulations[9,10] at the same temperature and pressures. We found excellent numerical agreement at the low pressure of 1 bar. At high pressures, we found minor differences between the results of both methods for $g(r)$ at relative distances $r>4$ Å. We attribute them to the neglect of spatial triplet-correlation effects within the present realization of CDM theory.[2]

We begin our study with a general formal CDM analysis of function $g(r)$ and the corresponding liquid structure function $S(k)$ of a strongly correlated normal Bose fluid (Sec. II). Assuming complete screening of particle exchange by strongly repulsive interactions at short relative distances, we specialize the formalism to deal with quantum Boltzmann liquids. Both algorithms are then applied to a numerical study of liquid *para*-hydrogen. Here and in Sec. III, we discuss the suppression of quantum-mechanical exchange effects and its consequences on the quasiparticle momentum distribution and excitation spectra. In Sec. IV, we investigate the off-diagonal elements of the one-body reduced density matrix, their spatial structure, and the interplay between particle exchange and phase-phase correlations. We further analyze the momentum distribution, the total kinetic energy, and the kinetic-energy distribution in momentum space. The formal CDM results are supported by numerical results on the hydrogen system. We conclude the paper with a summary and a brief outlook in Sec. V.

II. RADIAL DISTRIBUTION FUNCTION

The radial distribution function of a homogeneous normal system of N free or interacting bosons (in the thermodynamic limit, i.e., N and volume V to infinity, with particle-number density $\rho=N/V$ kept constant) may be decomposed into[1]

$$g(r) = 1 + G_{\mathrm{dd}}(r) + 2G_{\mathrm{de}}(r) + G_{\mathrm{ee}}(r). \tag{1}$$

The terms $G_{\mathrm{dd}}(r)$, $G_{\mathrm{de}}(r)$, and $G_{\mathrm{ee}}(r)$ in Eq. (1) represent the direct-direct (or dynamical) correlations, the direct-exchange, and the exchange-exchange portions, respectively. These components are induced by the interactions between and among the constituents of the fluid and by the particle exchange. CDM theory[1,2] provides explicit expressions and hypernetted-chain (HNC) relations for these correlation functions.

The sum (1) may be cast in the product form

$$g(r) = [1 + G_{\mathrm{dd}}(r)]F(r) \tag{2}$$

that gives a clean separation of dynamic and exchange effects. The exchange factor $F(r)$ involves the classical statistical factor $\Gamma_{\mathrm{cc}}(k)$ and (in diagrammatic HNC notation) nodal and elementary pieces associated with the exchange-correlation functions appearing in Eq. (1). CDM theory gives the explicit relation

$$F(r) = F_{\mathrm{cc}}^2(r) + [1 + N_{\mathrm{de}}(r) + E_{\mathrm{de}}(r)]^2 + N_{\mathrm{ee}}(r) + E_{\mathrm{ee}}(r), \tag{3}$$

with the cyclic exchange component

$$F_{\mathrm{cc}}(r) = \Gamma_{\mathrm{cc}}(r) + N_{\mathrm{cc}}(r) + E_{\mathrm{cc}}(r). \tag{4}$$

The optimization of all these functions for a specific normal Bose system within CDM theory may be achieved by solving the Euler-Lagrange equation [cf. Eq. (19) of Ref. 2]

$$\left[-\frac{\hbar^2}{m}\nabla^2 + v(r) + w(r) + v_{\mathrm{coll}}(r) + v_{\mathrm{qp}}(r)\right]\sqrt{g(r)} = 0. \tag{5}$$

This equation may be interpreted as an effective Schrödinger equation for the square root of the radial distribution function with energy eigenvalue zero at given temperature T and density ρ. Input quantity is the interparticle potential $v(r)$. Equation (5) involves the induced potential $w(r)$ and the effective potentials $v_{\mathrm{coll}}(r)$ and $v_{\mathrm{qp}}(r)$, which account for the coupling to the phonon and/or roton field and to the quasiparticle excitations, respectively. These components are functionals of the structure function $S(k)$ and of the occupation numbers $n_{\mathrm{coll}}(k)$ of the collective excitations and $n_{\mathrm{qp}}(k)$ of the quasiparticle excitations. In momentum space, the induced potential and the Fourier transform of the coupling term $v_{\mathrm{coll}}(r)$ read, respectively,

$$w(k) = -\frac{1}{2}\epsilon_0(k)[1 + 2S(k)][1 - S^{-1}(k)]^2 \tag{6}$$

and

$$v_{\mathrm{coll}}(k) = -\frac{1}{2}\epsilon_0(k)\{[1 + 2n_{\mathrm{coll}}(k)]^2 - 1\}S^{-2}(k), \tag{7}$$

where $\epsilon_0(k)=\hbar^2k^2/2m$ is the kinetic energy of a single boson of mass m. The effective potential $v_{\mathrm{qp}}(r)$ can be evaluated with the help of the CDM algorithm.[1,2]

For free bosons, portions $G_{\mathrm{dd}}(r)$ and $G_{\mathrm{de}}(r)$ are identically zero and the quantum-mechanical exchange-correlation function $G_{\mathrm{ee}}(r)$ is completely determined by the cyclic exchange correlations described by the spatial distribution $G_{\mathrm{cc}}(r)$. Thus, the decompositions (1)–(4) specialize to

$$g(r) = F(r) = 1 + G_{\mathrm{ee}}(r) = 1 + F_{\mathrm{cc}}^2(r) \tag{8}$$

and

$$F_{\mathrm{cc}}(r) = \Gamma_{\mathrm{cc}}(r) + N_{\mathrm{cc}}(r). \tag{9}$$

In this case, the Schrödinger equation (5) can be analytically solved since the potentials $v(r)$ and $v_{\mathrm{coll}}(r)$ are identically zero. The optimal functions $g(r)$ and $F_{\mathrm{cc}}(r)$ are determined by the familiar Bose distribution

$$F_{\mathrm{cc}}(k) = \Gamma_{\mathrm{cc}}(k)[1 - \Gamma_{\mathrm{cc}}(k)]^{-1}, \tag{10}$$

with

$$\Gamma_{\mathrm{cc}}(k) = \exp\{-\beta[\epsilon_0(k) - \mu_0]\}. \tag{11}$$

The corresponding chemical potential μ_0 follows from the condition $F_{\mathrm{cc}}(r=0)=1$ that takes account of the total number N of constituents of the Bose gas. Thus, a normal free Bose

TABLE I. Listed are interpolated experimental data (Ref. 13) of particle-number densities ρ of liquid *para*-hydrogen corresponding to the temperature $T=16.5$ K and three different pressures.

Pressure (bar)	1	40	80
Density ($Å^{-3}$)	0.02235	0.02327	0.02413

gas is completely characterized by circular exchange correlations. The radial distribution function $g(r)$ coincides with function $F(r)$ and is positive at any finite relative distance. There is no screening of exchange effects, since for noninteracting particles the first factor in Eq. (2) is unity. However, in dynamically correlated systems, this factor can be substantially altered depending on the short-range properties of the interaction potential since the correlation function $G_{dd}(r)$ may be negative and *not* small. For example, the potential $v(r)$ for liquid *para*-hydrogen[11] is strongly repulsive at relative distances $r<2$ Å, and thus, one has practically $G_{dd}(r)=-1$ in this region of coordinate space. The repulsion between and among the H_2 molecules in the liquid prevents close encounters and, consequently, the exchange of particles is suppressed since the function $F(r)-1$ is also of short range. It practically vanishes outside the repulsive region at temperatures close to the triple point. Under such thermodynamic conditions, the Bose system can be characterized by

$$[1+G_{dd}(r)][F(r)-1]\simeq 0. \tag{12}$$

The expressions (1) and (2) for the radial distribution function specialize, therefore, to

$$g(r)=1+G_{dd}(r). \tag{13}$$

Liquid *para*-hydrogen close to the triple point temperature is a typical member of this class of quantum Boltzmann liquids. More explicitly, we may characterize these quantum systems within CDM theory by the properties $G_{de}(r)\simeq 0$, $G_{ee}(r)\simeq 0$, $F(r)\simeq 1$, and $v_{qp}(r)\simeq 0$. With these specializations, the application of the CDM formalism reduces to a rather elementary numerical task. The Euler-Lagrange equation (5) may be solved by employing the techniques devised in Ref. 12.

We have performed a detailed numerical calculation of the radial distribution function $g(r)$ and the associated structure function $S(k)$ for the hydrogen liquid at $T=16.5$ K and pressures of 1, 40, and 80 bar. The corresponding particle-number densities are interpolated experimental data[13] and are listed in Table I. We have solved Eq. (5) by adopting the Silvera-Goldman potential[11] as input *without* assuming the presence of particle-screening effects. In a separate calculation, we have assumed at the outset that the hydrogen system is a perfect quantum Boltzmann liquid; i.e., we have set $F(r)$ to unity and $v_{qp}(r)$ to zero. The numerical results of the two differing procedures agree excellently. The agreement, therefore, confirms that liquid *para*-hydrogen has, indeed, the properties of a quantum Boltzmann liquid.

Figures 1 and 2 represent our numerical results on function $g(r)$ at $T=16.5$ K and pressures of 1 and 80 bar. We see that the repulsive part of the Silvera-Goldman potential prohibits the molecules from entering the hard-core region, $r<2$ Å, where the exchange factor $F(r)$ differs from unity. As expected, at high pressures (up to 80 bar), the shell structure of the spatial correlations is distinctly more pronounced than the structure found at low pressure.

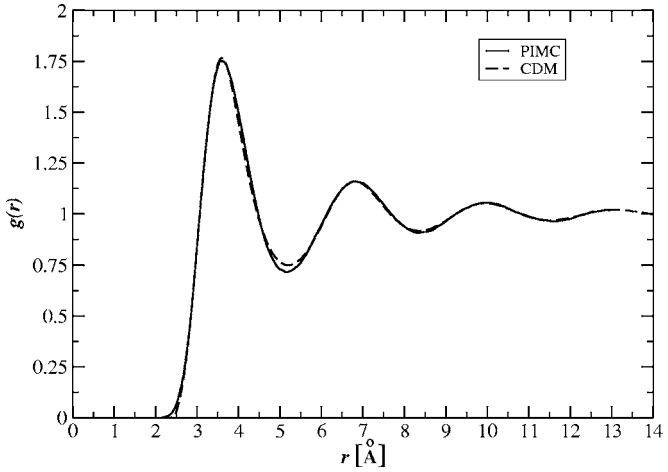

FIG. 1. Numerical results on the radial distribution function $g(r)$ of liquid *para*-hydrogen at temperature $T=16.5$ K and pressure of 1 bar: calculated by CDM theory (broken line) and compared with results by PIMC simulations (solid line).

To check the accuracy of the CDM results, we have performed PIMC simulations[9,10] for the radial distribution function at the same temperature and pressures. For comparison, these results on function $g(r)$ are also displayed in Figs. 1 and 2. At the pressure of 1 bar, there is very good agreement between the results by CDM and the simulation results. At higher pressures, small differences begin to appear. At 80 bar, the stochastic results show somewhat larger amplitudes of the oscillations in the shell structure beyond the main maximum at about $r=3.5$ Å. The very small differences may be caused by, at present, the neglected elementary contribution in the adopted HNC/0 approximation and/or by ignoring triplet factors in the employed ansatz for the gen-

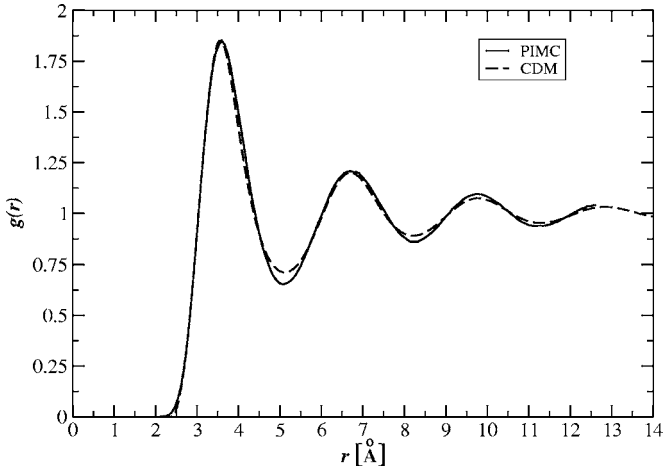

FIG. 2. Same as Fig. 1 but at high pressure (80 bar). The PIMC results show a more pronounced shell structure beyond the main maximum at about 3.5 Å than the results of CDM theory.

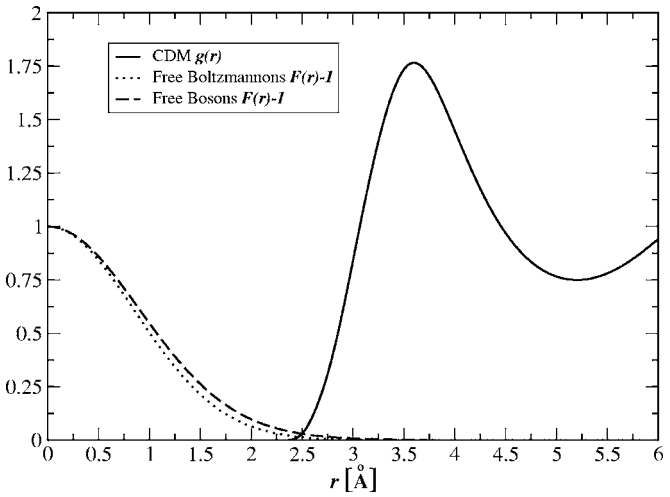

FIG. 3. CDM results on the exchange factor $F(r)-1$ of Eq. (3) for liquid *para*-hydrogen at $T=16.5$ K and pressure of 1 bar compared with the corresponding dynamical factor $1+G_{\mathrm{dd}}(r)$ [Eq. (13)]. The exchange functions do not overlap with function $g(r)$, thus confirming the validity of the Boltzmann condition [Eq. (12)].

eration of the N-body density matrix.[1,2] To study this subtle matter systematically, one has to generalize the CDM formalism by replacing the currently employed Jastrow ansatz for the N-body density matrix with a trial Feenberg form.[14,15]

We point out that our results on function $g(r)$ are comparable with PIMC results reported in Ref. 16.

To demonstrate the complete screening of exchange correlations in liquid *para*-hydrogen, we have plotted our CDM results on functions $F(r)-1$ and $g(r)=1+G_{\mathrm{dd}}(r)$ at the pressure of 1 bar in Fig. 3. The broken (dotted) line displays the results on the exchange function $F(r)$ assuming Bose (Boltzmann) statistics. The dynamical (de) and (ee) contributions to this function do not increase the screening range since they are extremely small at distances $r>2.5$ Å. We recognize, in agreement with Eq. (12), that for all practical considerations $F(r)-1$ and $g(r)$ do not overlap as it should be for a quantum Boltzmann liquid.

The liquid structure function $S(k)$ is evaluated in CDM theory as well as in the PIMC procedure by numerical integration of the results for $g(r)$,

$$S(k) = 1 + \rho \int [g(r) - 1] e^{-i\mathbf{kr}} d\mathbf{r}. \tag{14}$$

The numerical results on $S(k)$ for the hydrogen liquid at $T=16.5$ K and high pressure of 80 bar are displayed in Fig. 4. The PIMC results on function (14) are calculated without adopting any standard tail corrections.[17] The large oscillations of the stochastic data compared with the results by CDM are artifacts of the simulations which have to be done in a box of relatively small size. This restriction is dictated by the methodological limitations of the stochastic method. To eliminate the spurious oscillations, the PIMC approach utilizes Verlet's recipe[17] by smoothly extrapolating the radial distribution function $g(r)$ to large enough relative distances r via a damped oscillatory function.[16] No extrapolation is

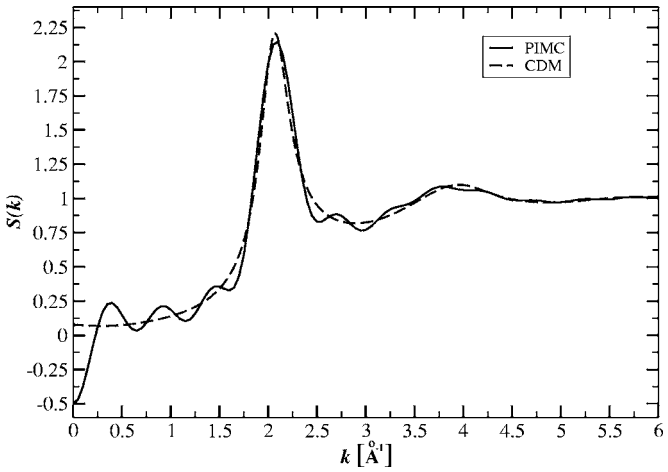

FIG. 4. Theoretical structure function $S(k)$ of liquid *para*-hydrogen at $T=16.5$ K and high pressure (80 bar). The broken line shows numerical results by CDM. They are compared with results of PIMC simulations (solid line) without adopting the standard tail corrections prescribed in Ref. 16 (see text).

needed in CDM theory since the Euler-Lagrange equation (5) can and has been solved in a sufficiently large interval of relative distances $0 \leqslant r \leqslant 330$ Å. We note that the PIMC data for the structure function $S(k)$ given in Ref. 16 display a main peak of magnitude $S(k_{\mathrm{max}}) \simeq 2.17$ at $k_{\mathrm{max}} \simeq 2.1$ Å^{-1}. These data agree very well with our numerical results on $S(k)$ by CDM and PIMC.

CDM theory is therefore an efficient and accurate tool for investigating microscopic properties of quantum Boltzmann liquids. In particular, we may derive reliable theoretical data on the isothermal compressibility and sound velocity of the system by calculating $S(k)$ in the limit of vanishing wave number k (for further discussions see Sec. IV).

The dependence of the liquid structure function of the H_2 liquid at temperature $T=16.5$ K on the particle density (or pressure) is represented in Fig. 5. Plotted are CDM results at three pressures (1, 40, and 80 bar). The main peak increases with increasing pressure as expected.

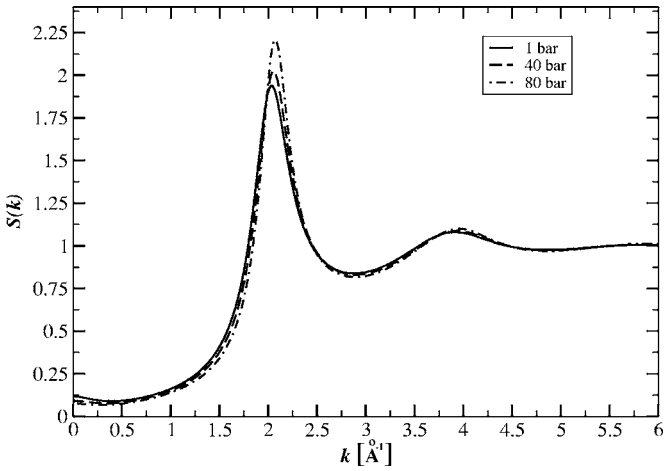

FIG. 5. CDM results on the liquid structure function $S(k)$ at pressures of 1, 40, and 80 bar. The peak height increases with increasing pressure as expected.

III. QUASIPARTICLES AND COLLECTIVE EXCITATIONS

Cyclic exchange correlations in normal Bose systems develop long-range order at sufficiently low temperatures and trigger the transition to a Bose-Einstein condensed phase. These correlations play, therefore, a particular role in the CDM formalism. They are embodied in the cyclic correlation function $G_{cc}(r)$ and the associated exchange structure function $S_{cc}(k)$. CDM theory provides the product decomposition[1,2]

$$G_{cc}(r) = [1 + G_{dd}(r)]F_{cc}(r), \tag{15}$$

with the cyclic exchange factor $F_{cc}(r)$ defined in Eq. (4). Its dimensionless Fourier transform represents function $S_{cc}(k)$. Formal analysis reveals that we may write in momentum space [cf. Eqs. (4.8) and (4.10) of Ref. 1]

$$S_{cc}(k) = [\Gamma_{cc}(k) + X_{cc}(k)][1 - \Gamma_{cc}(k) - X_{cc}(k)]^{-1}. \tag{16}$$

The explicit form (16) involves the statistical factor $\Gamma_{cc}(k)$ and the non-nodal portion $X_{cc}(k)$ of the exchange structure function. For free Bose gases, $X_{cc}(k)$ is identically zero and expression (16) specializes to the familiar result (10) with the statistical factor (11). At the Bose-Einstein transition, the Bose function diverges at vanishing wave number k, signaling the onset of long-range order of particle exchange in coordinate space. For correlated normal Bose fluids, function $X_{cc}(k)$ differs from zero and the transition to the condensed phase is indicated by the property $\Gamma_{cc}(0)+X_{cc}(0)=1$ at $k=0$.

In thermodynamic phase space, a correlated Bose liquid must, therefore, be sufficiently far from the region of the condensed states in order to exhibit the properties of a quantum Boltzmann liquid. The cyclic exchange correlations in coordinate space must be of appropriate short range, otherwise they cannot be screened by the repulsive particle-particle interaction at short relative distances. Complete screening is achieved if the condition

$$[1 + G_{dd}(r)]F_{cc}(r) \simeq 0 \tag{17}$$

is met. In this case, the cyclic exchange-correlation function $G_{cc}(r)$ and the structure function $S_{cc}(k)$ vanish or must be negligibly small compared to unity. According to Eq. (16), we can further conclude that the non-nodal dynamic correlations completely cancel the kinematic statistical distribution, $\Gamma_{cc}(k)+X_{cc}(k)=0$.

CDM theory addresses the quasiparticle concept for correlated normal Bose fluids by introducing the associated momentum distribution[1,2]

$$n_{qp}(k) = \Gamma_{cc}(k)[1 + S_{cc}(k)]. \tag{18}$$

Evidently, for quantum Boltzmann liquids, expression (18) reduces to

$$n_{qp}(k) = \Gamma_{cc}(k). \tag{19}$$

Since the optimal statistical function $\Gamma_{cc}(k)$ turns out to be of Gaussian form, the quasiparticle momentum distribution of a quantum Boltzmann liquid is represented by the familiar classical expression

$$n_{qp}(k) = \rho\lambda^3 \exp[-\beta\epsilon_0(k)], \tag{20}$$

with the thermal wavelength $\lambda=(2\pi\beta\hbar^2/m)^{1/2}$. For liquid *para*-hydrogen at $T=16.5$ K, its value is $\lambda=3.03$ Å. The Fourier transform

$$n_{qp}(r) = \exp\left[-\pi\left(\frac{r}{\lambda}\right)^2\right] \tag{21}$$

may be appropriately called the one-body reduced density matrix that corresponds to the quasiparticle momentum distributions (19) and (20). Thus, the quasiparticles are distinguishable and noninteracting objects with a kinetic energy $\epsilon_0(k)$ and obey classical Boltzmann statistics. The average kinetic energy of all N quasiparticles is, therefore, given by the classical result $E_0=\frac{3}{2}Nk_BT$. These properties distinctively differ from those of the actual constituents in a quantum liquid. For example, the momentum distribution $n(k)$ of a H_2 molecule in liquid *para*-hydrogen differs from expression (20). The particle properties will be analyzed in Sec. IV. There we show that the quasiparticle energy E_0 is only one portion that contributes to the total kinetic energy of the fluid.

In addition to the quasiparticle excitations just discussed, a correlated Bose liquid may also support collective excitations with zero chemical potential and energy $\omega_{coll}(k)$ at momentum $\hbar\mathbf{k}$. Their occupation-number density in momentum space is[1,2]

$$n_{coll}(k) = \{\exp[\beta\omega_{coll}(k)] - 1\}^{-1}. \tag{22}$$

At the present level of development of CDM theory, we determine the dispersion law of the collective excitations via the generalized Feynman equation[1,12,18]

$$\omega_{coll}(k) = \epsilon_0(k)S^{-1}(k)\coth\left[\frac{1}{2}\beta\omega_{coll}(k)\right] \tag{23}$$

in conjunction with the renormalized Bogoliubov equation

$$\omega_{coll}^2(k) = \epsilon_0(k)[\epsilon_0(k) + 2v_{ph}(k)]. \tag{24}$$

This equation involves the Fourier transform $v_{ph}(k)$ of the so-called particle-hole potential[12]

$$v_{ph}(r) = g(r)v(r) + [g(r) - 1][w(r) + v_{coll}(r)] + \frac{\hbar^2}{m}[\nabla\sqrt{g(r)}]^2, \tag{25}$$

where the Fourier transforms $w(k)$ of $w(r)$ and $v_{coll}(k)$ of $v_{coll}(r)$ are given by Eqs. (6) and (7), respectively. Expression (25) and the Bogoliubov equation (24) are then employed within a systematic iteration procedure to calculate the numerical dependence of the energy spectrum $\omega_{coll}(k)$ on wave number k. Relation (23) ignores the so-called backflow effects at atomic wavelengths. However, for liquid *para*-hydrogen, such backflow corrections are of little interest, since the experimentally observed collective excitations at large wave numbers k are strongly damped.[19]

Figure 6 displays the numerical results on the energy branch $\omega_{coll}(k)$ for the hydrogen liquid at $T=16.5$ K and pressures of 1, 40, and 80 bar. The theoretical results are compared with available experimental data.[19] The theoretical dispersion law is of the typical phonon and/or roton form. It

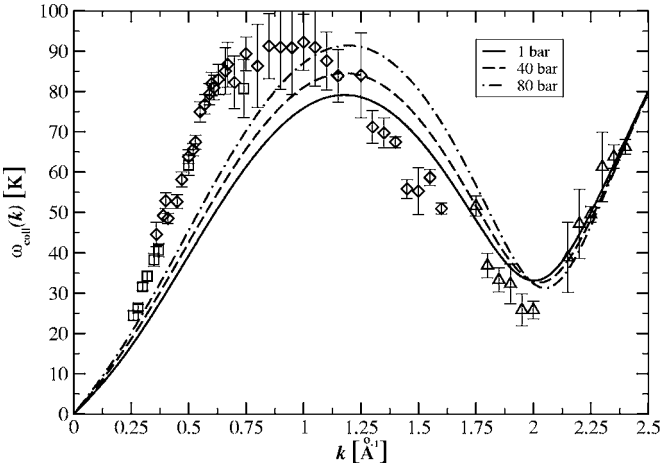

FIG. 6. Theoretical energy $\omega_{coll}(k)$ of the collective excitations in liquid *para*-hydrogen at $T=16.5$ K and pressures of 1, 40, and 80 bar calculated from Eq. (23) within CDM theory. The results are compared with available experimental data of Ref. 19 measured at 1 bar (vertical lines indicate experimental error bars).

is completely determined by the dynamical correlations and not affected by particle exchange in the hydrogen fluid. This is apparent from Eq. (23), since the spectrum has a simple relationship with the liquid structure function $S(k)$ and therefore also with the radial distribution function $g(r)$ that only depends on the dynamical correlations $G_{dd}(r)$ [Eq. (13)]. However, it may be that the theoretical results presented have to be corrected if so-called backflow effects are incorporated in the CDM approach. They are neglected in the present realization of the CDM theory.

A comparison between the theoretical results and the experimental findings is rather intricate. Reference 19 provides a detailed discussion of the inherent problems from the experimental point of view. It is clear that the CDM results and the data extracted from measurements should be close to each other at wave numbers k where damping effects are minimal, i.e., near the roton minimum and in the hydrodynamic regime of small k. In the other momentum ranges, the experimental data are not comparable to the present theoretical results, since the former data describe quantities that are dressed by the damping and the latter ones correspond to deltalike peaks.

Concentrating on the properties at low wave numbers, we see from Fig. 5 of Ref. 19 that our CDM results agree well with the theoretical results of simulations reported in Ref. 19 (open circles in Fig. 5 therein). The linear phonon spectrum $\omega_{coll}(k)=\hbar c_T k$ calculated by CDM yields the theoretical isothermal speed of sound $c_T(\rho)$ (see Table II).

We refrain from a detailed comparison of our theoretical results with experimental data extracted from neutron-scattering measurements since the hydrodynamic regime, where $c_T(\rho)$ could be well determined, is far below the smallest wave number, $k=0.3$ Å^{-1}, reached by experiment.

We have also listed in Table II the corresponding theoretical results on the isothermal compressibility $\kappa_T=[mc_T^2\rho]^{-1}$ in the hydrodynamic regime of liquid *para*-hydrogen. Thermodynamic relations further permit extracting numerical data

TABLE II. Theoretical results by CDM theory on the isothermal speed of sound c_T, the isothermal compressibility κ_T, and the value $S(0)$ of the structure function $S(k)$ at zero wave number k. Numbers are calculated at temperature $T=16.5$ K and three pressures. Results on $S(0)$ are derived by employing two different numerical procedures, (a) and (b). For comparison, we have also listed numerical data at $T=17.1$ K reported in Ref. 16. For a detailed discussion, see the corresponding text.

$T=16.5$ K			
Pressure (bar)	1	40	80
c_T (m/s)	772	872	957
κ_T (1/bar)	224	169	135
$S(0)$ (a)	0.1221	0.1005	0.0909
$S(0)$ (b)	0.1143	0.0896	0.0743
	$T=17.1$ K		
Pressure (bar)	16.2	29.9	
$S(0)$ from Ref. 16	0.065	0.059	

on $S(k=0)$ from the phonon speed in the hydrodynamic region via $S(0)=\rho T\kappa_T$ and also from the particle-hole potential (25) through the generalized Bogoliubov equation (24) in the limit of vanishing wave number, namely, $S(0)=T/v_{ph}(k=0)$. These data are also reported in Table II as results (a) and (b), respectively. The difference of about 10%–15% is presumably due to the accumulation of small numerical inaccuracies in our numerical iteration procedure. Data reported in Ref. 16 on $S(0)$ are smaller than our present results. These theoretical and experimental problems deserve further studies in their own right. Here, they would lead us away from the primary topic of the structural effects of particle exchange in quantum fluids.

IV. PHASE-PHASE CORRELATION FUNCTION

In contrast to the diagonal elements of the two-body reduced density matrix, the off-diagonal elements of the one-body density depend not only on dynamical correlations and particle exchange but also on spatial correlations between and among the phase factors of the single-particle wave functions which contribute to the full N-body density matrix of the system. The latter correlations are, of course, absent in free Bose gases since the phases are uncorrelated in an N-particle state represented by a product of N single-particle factors.

The spatial phase-phase correlations existing in a correlated Bose fluid, in particular, in a quantum Boltzmann liquid, are characterized within the CDM algorithm by the distribution function $P(r)$ normalized to unity at $r=0$. The magnitude of these correlations is measured by the strength parameter p_0. Their relation to the off-diagonal elements $n(r)$ of the one-body reduced density matrix reads[20]

$$n(r)=N_0(r)\exp\{p_0[P(r)-1]\}. \tag{26}$$

The product (26) represents a generic decomposition that has been analyzed in detail in Ref. 20 by employing a diagram-

matic classification algorithm. Function $N_0(r)$ is entirely described by cyclic (cc) contributions. For noninteracting bosons, its Fourier transform is represented by the familiar Bose distribution function $\Gamma_{cc}(k)\{1-\Gamma_{cc}(k)\}^{-1}$ with a Gaussian form $\Gamma_{cc}(k)=\exp\{\beta[\mu_0-\epsilon_0(k)]\}$. For an interacting Bose system, the cyclic exchange factor $N_0(r)$ is, of course, dressed by dynamical insertions. The exponential factor, in contrast, is represented by dynamical direct-direct diagrams and generated by the particle-particle interactions. Reference 20 gives an explicit account of the (dd) contributions to function $Q(r)=Q(0)P(r)$ with $\ln n_c=Q(0)=-p_0$. Functions $N_0(r)$ and $P(r)$ are suitably normalized to unity at $r=0$.

The cyclic exchange function $N_0(r)$ may be calculated by employing the CDM and/or HNC decomposition

$$N_0(r)=\Gamma_{cc}(r)+N_c(r)+E_c(r). \tag{27}$$

Reference 20 reports a detailed diagrammatic derivation of expression (27) in terms of the statistical function $\Gamma_{cc}(r)$, the nodal component $N_c(r)$, and the elementary portion $E_c(r)$. Similarly, the short-ranged correlation function $P(r)$ may be expressed by CDM in the form

$$-p_0P(r)=N_{pdd}(r)+E_{pdd}(r). \tag{28}$$

The momentum distribution $n(k)$ of a single particle in the liquid may be calculated as the Fourier transform of expression (26). The kinetic-energy distribution in momentum space is given by the product $\epsilon_0(k)n(k)$. The total kinetic energy E_{kin} of the fluid then follows by summing over all momenta. However, it is more illuminating to employ the equivalent relation

$$\frac{E_{kin}}{N}=-\frac{\hbar^2}{2m}[\nabla^2 n(r)]_{r=0}. \tag{29}$$

Inserting the structural result (26) in Eq. (29) and assuming that functions $N_0(r)$ and $P(r)$ depend quadratically on r at small relative distances, we arrive at the energy decomposition

$$E_{kin}=E_0+p_0E_p, \tag{30}$$

with the portions

$$\frac{E_0}{N}=-\frac{\hbar^2}{2m}[\nabla^2 N_0(r)]_{r=0} \tag{31}$$

and

$$\frac{E_p}{N}=-\frac{\hbar^2}{2m}[\nabla^2 P(r)]_{r=0}. \tag{32}$$

Equations (31) and (32) provide a clean separation of exchange effects from phase-phase correlation effects.

Before turning to an analysis of function $n(r)$ and related quantities (27)–(32) for the class of quantum Boltzmann liquids, we look for comparison at the case of a free normal Bose gas. Here, the strength p_0 vanishes identically and the exchange factor $N_0(r)$ specializes to the Fourier transform of function (10) with the statistical factor $\Gamma_{cc}(k)$ of Eq. (11). Thus, the one-body reduced density matrix (26) coincides with the quasiparticle analog $n_{qp}(r)$. The total kinetic energy per particle is then completely given by the energy portion (31).

TABLE III. Theoretical results by CDM and experimental results of Ref. 8 on various quantities characterizing quantum properties of liquid *para*-hydrogen at $T=16.5$ K and pressures of 1, 40, and 80 bar. Shown are data for the total kinetic energy per particle, E_{kin}/N, the quantum component p_0E_p/N, the correlation strength p_0, the correlation length λ_p, the wavelength λ_G of the classical thermal Gauss distribution, and the total energy shift Δ_- induced by the phase-phase correlation embodied in the kinetic-energy distribution.

Theoretical data fit (CDM)			
Pressure (bar)	1	40	80
E_{kin}/N (K)	62.7±0.4	65.5±0.5	69.6±0.5
p_0E_p/N (K)	37.9±0.4	40.7±0.5	44.9±0.5
p_0	1.83	1.91	2.06
λ_p (Å)	3.31	3.31	3.31
λ_G (Å)	1.90	1.86	1.81
Δ_- (K)	−9.4	−9.5	−9.8
Experimental data fit (cf. Ref. 8)			
E_{kin}/N (K)	67.78±0.26	73.49±0.40	77.51±0.39
p_0E_p/N (K)	43.03±0.26	48.74±0.40	52.76±0.39
λ_G (Å)	1.84	1.76	1.71
Δ_- (K)	−6.0	−5.0	−5.0

By screening of particle exchange in quantum Boltzmann liquids, the short-ranged quantities $N_c(r)$ and $E_c(r)$ in decomposition (27) may be ignored. Thus, we are left with

$$N_0(r)\simeq\Gamma_{cc}(r)\simeq\exp\left[-\pi\left(\frac{r}{\lambda}\right)^2\right]. \tag{33}$$

Consequently, quantity (31) just yields the familiar classical result for the total energy of distinguishable free Boltzmann particles,

$$\frac{E_0}{N}=\frac{3}{2}\frac{\hbar^2}{m}\frac{2\pi}{\lambda^2}=\frac{3}{2}k_BT. \tag{34}$$

We can, therefore, conclude that the increase in kinetic energy of a quantum Boltzmann liquid compared with its classical counterpart originates from the presence of quantum-mechanical phase-phase correlations.

Table III lists numerical results on the total kinetic energy per particle, E_{kin}/N, and the energy contribution per particle, p_0E_p/N, associated with the phase-phase correlations in liquid *para*-hydrogen at $T=16.5$ K and at the pressures of 1, 40, and 80 bar. The theoretical data on the total kinetic energy are results of PIMC simulations. The classical energy portion (34) has the numerical value $E_0/N=24.75$ K. The correlation component p_0E_p is given by the difference $E_{kin}-E_0$. The theoretical results may be compared with experimental results extracted from recent neutron cross-section data by an appropriate fitting procedure at the same temperature and pressures.[8] The results differ typically by about 10%–15%. Our theoretical results on the total kinetic energy per particle are close to the results given for this quantity in Ref. 21.

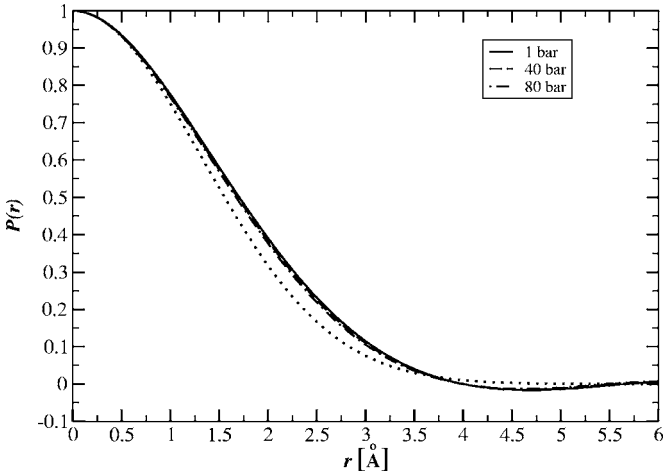

FIG. 7. Results by CDM theory on the phase-phase correlation function $P(r)$ of liquid H_2 at temperature $T=16.5$ K. The correlations are practically independent of pressure and well represented at short relative distances by a Gaussian function with correlation length λ_p. The dotted curve displays the results for $P(r)$ obtained from the limit (35) with $\lambda_p=3.31$ Å (Table III).

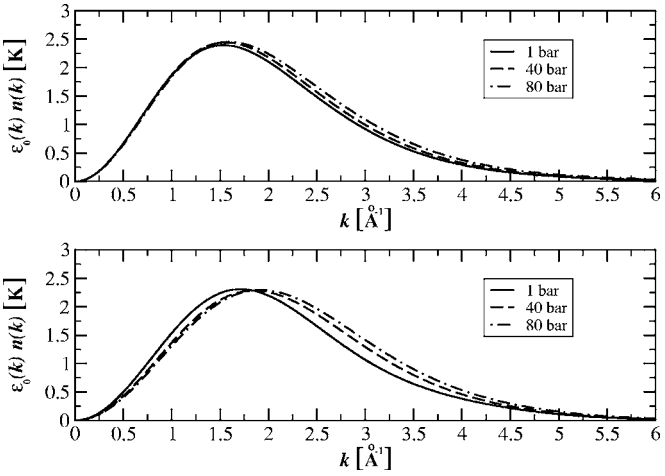

FIG. 8. Kinetic-energy distribution $\epsilon_0(k)n(k)$ of liquid H_2 at temperature $T=16.5$ K and pressures of 1, 40, and 80 bar. Upper frame displays the results by CDM theory; lower frame shows corresponding experimental data of Ref. 8.

The phase-phase correlation function $P(r)$ for the hydrogen liquid is calculated by employing the CDM algorithm of Ref. 20 in conjunction with the HNC/0 approximation that neglects the elementary contribution $E_{\mathrm{pdd}}(r)$ appearing in expression (28). The numerical results are plotted in Fig. 7. Function $P(r)$ is almost independent of pressure and well represented at short relative distances by a Gaussian distribution with a correlation length λ_p,

$$P(r) \simeq \exp\left[-\pi\left(\frac{r}{\lambda_p}\right)^2\right] \quad \text{as } r \to 0. \tag{35}$$

For liquid *para*-hydrogen at $T=16.5$ K, we find the numerical value $\lambda_p \approx 3.31$ Å. Thus, the phase-phase correlations have a larger spatial range compared with the thermal wavelength $\lambda=3.03$ Å associated with the quasiparticles. With Eq. (35) the total kinetic energy (30) may be cast in the explicit form

$$\frac{E_{\mathrm{kin}}}{N} = \frac{E_0}{N}\left[1 + p_0\left(\frac{\lambda}{\lambda_p}\right)^2\right]. \tag{36}$$

Equation (36) permits a straightforward calculation of the strength factor p_0 by inserting our numerical results on the energies E_{kin} and E_0 and on the parameters λ and λ_p. The theoretical results are presented in Table III. We note that the numerical results on the parameters λ_p and p_0 depend sensitively on the numerical determinations of the curvature of function $P(r)$ at short relative distances r.

We may extract more detailed information on quantum effects in a quantum Boltzmann liquid by a formal and numerical analysis of the distribution of the kinetic energy in momentum space. The dependence of function $\epsilon_0(k)n(k)$ on wave number k for liquid *para*-hydrogen is represented in Fig. 8. The theoretical results (upper frame) may be compared with the corresponding experimental results (lower frame) taken from Ref. 8. The CDM calculations yield a slightly higher maximum of the theoretical energy distribution of approximately 2.4 K at a wave number $k_{\max} \simeq 1.5$ Å^{-1} than is experimentally derived ($\simeq 2.3$ K) at $k_{\exp} \simeq 1.7$ Å^{-1}. The maxima are almost independent of pressure. However, as expected, the theoretical results as well as the experimental data show an increase of kinetic energy at larger wave numbers if the pressure is raised toward the solidification point.

We stress that this analysis of particle-exchange effects and its comparison with experimental data require a numerical calculation *and* an experimental determination of the momentum distribution

$$n(k) = \rho \int n(r) e^{-i\mathbf{kr}} d\mathbf{r}. \tag{37}$$

Knowledge of the value of the total kinetic energy of the system is, therefore, not enough. For this reason, we compare the results of CDM theory with available data on $n(k)$ from Ref. 8 and also employ, for consistency, the results on the total kinetic energy reported in this publication. There are some published experimental values for the kinetic energy that are closer to our theoretical results. Reference 21 reports (see Tables II–IV therein) three "model-dependent" determinations $E_{\mathrm{kin}}/N=63.5\pm0.4$, 65.0 ± 0.2, and 64.2 ± 0.3 K. Further experimental and PIMC data for a dense hydrogen system are presented in Ref. 22.

The quantum effects embodied in function (37) become apparent by comparing with the corresponding classical Maxwell-Gauss kinetic-energy distribution, $\epsilon_0(k)n_G(k)$. The classical momentum distribution $n_G(k)$ is of the familiar Gaussian form

$$n_G(k) = \rho\lambda_G^3 \exp[-\beta\epsilon_0(k)], \tag{38}$$

with an effective wavelength λ_G defined by

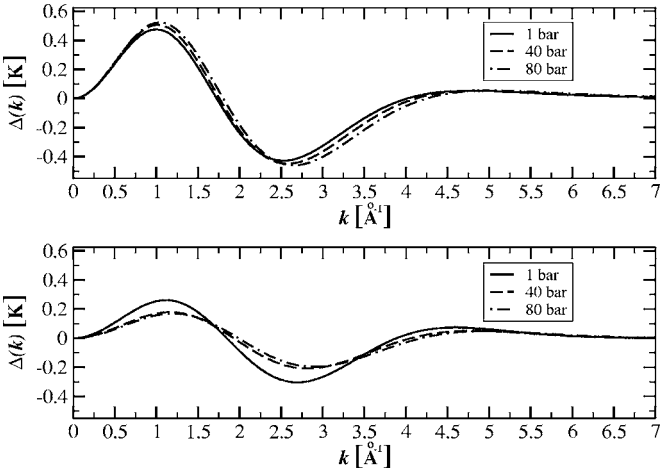

FIG. 9. Displayed are numerical results of CDM theory on the difference $\Delta(k)$ [cf. Eq. (40)] that measures the quantum-mechanical deviation from the corresponding classical Maxwell-Gauss energy distribution for the hydrogen system at $T=16.5$ K and pressures of 1, 40, and 80 bar. Upper frame: Theoretical results by CDM; lower frame: experimental data of Ref. 8 (see the discussion in Sec. IV).

$$\lambda_G = \left(\frac{E_0}{E_{\rm kin}}\right)^{1/2} \lambda. \tag{39}$$

Relation (39) ensures that the total kinetic energy E_G associated with the classical Gaussian distribution (38) is equal to the total kinetic energy (29) and (30) of the correlated Boltzmann liquid. Insertion of the theoretical values for the quantities E_0, $E_{\rm kin}$, and λ for the hydrogen liquid at $T=16.5$ K yields the data shown in Table III at pressures of 1, 40, and 80 bar.

The difference

$$\Delta(k) = \epsilon_0(k)[n(k) - n_G(k)] \tag{40}$$

provides a quantitative measure of the deviation from the classical Maxwell-Gauss distribution for a quantum Boltzmann liquid. Numerical results on function (40) calculated for the hydrogen liquid by CDM are displayed in Fig. 9 (upper frame). Experimental results are also shown in this figure (lower frame).

CDM theory and experiment demonstrate significant deviations from the classical energy distribution characterized by $\Delta(k)=0$. In both cases, quantum-mechanical zero-point fluctuations shift kinetic-energy portions from an intermediate region of momenta centered at wave number $k \simeq 2.5$ Å^{-1} and where $\Delta(k)<0$ to smaller wave numbers located around $k \simeq 1$ Å^{-1}. The effect is less pronounced in the results extracted from experiment. At the pressure of 1 bar, the total energy shift from the negative region, $\Delta(k)<0$, amounts to $\Delta_- \simeq -9.4$ K as calculated by CDM, in contrast to a value of about $\Delta_- \simeq -6.7$ K extracted from experimental data (Table III). At the present level of numerical accuracy as well as of the experimental precision of measurement, this discrepancy is acceptable but should await more refined investigations in the future.

V. CONCLUSIONS AND OUTLOOK

CDM theory of strongly correlated normal Bose fluids has been employed to analyze the spatial correlations and structure of quantum Boltzmann liquids. The general formalism has been properly specialized to deal with such quantum many-body systems. The theory has been applied to a detailed numerical study of microscopic properties of liquid *para*-hydrogen close to the triple point temperature.

We have investigated dynamical correlations, statistical correlations, particle-exchange effects, phase-phase correlations, momentum distributions, kinetic-energy distributions, and properties of excitations. The results demonstrate that liquid *para*-hydrogen, in the region of phase space considered, behaves like a typical quantum Boltzmann liquid.

Such systems exhibit characteristic properties: (i) complete screening of particle-exchange correlations in the diagonal elements $g(r)$ of the two-body reduced density matrix, (ii) distinguishability of quasiparticles moving with kinetic energy $\epsilon_0(k)$, (iii) classical Gaussian dependence on relative distance of the exchange factor $N_0(r)$ appearing in the one-body reduced density-matrix elements $n(r)$, (iv) an increase of the total kinetic energy $E_{\rm kin}$ caused by phase-phase correlations, and (v) quantum-mechanical deviations of the kinetic-energy distribution in momentum space from the classical Maxwell-Gauss dependence $\epsilon_0(k)n_G(k)$ on wave number k.

Reported here are detailed numerical results on the most interesting physical properties of the hydrogen liquid at a temperature $T=16.5$ K and in a range of particle densities. The numerical results on the kinetic-energy distribution and related functions have been compared with experimental data measured under the same thermodynamic conditions.

CDM theory may be employed to study the properties of other strongly correlated Bose systems and, in particular, of the more specialized quantum Boltzmann liquids such as liquid deuterium or helium under appropriate thermal conditions. In the case of liquid helium, we could further analyze the transition from complete screening of particle exchange to partial screening at lower temperatures and the disappearance of screening close to the Bose-Einstein condensation line.

Some efforts are required to proceed with CDM theory to a quantitatively reliable analysis of strongly correlated Bose liquids in the Bose-Einstein condensed phase at elevated temperatures close to the transition to the normal phase. CDM theory provides adequate analytic tools for this task.[2,23] Encouraging numerical studies on superfluid helium toward this goal have been reported in Refs. 2 and 24.

[1] G. Senger, M. L. Ristig, C. E. Campbell, and J. W. Clark, Ann. Phys. (N.Y.) **218**, 160 (1992).
[2] T. Lindenau, M. L. Ristig, J. W. Clark, and K. A. Gernoth, J. Low Temp. Phys. **129**, 143 (2002).
[3] E. Feenberg, *Theory of Quantum Fluids* (Academic, New York, 1969).
[4] J. W. Clark and P. Westhaus, Phys. Rev. **141**, 833 (1966).
[5] E. Krotscheck, in *Microscopic Quantum Many-Body Theories and Their Applications*, edited by J. Navarro and A. Polls, Lecture Notes in Physics Vol. 510 (Springer-Verlag, Berlin, 1998).
[6] M. L. Ristig and J. W. Kim, Phys. Rev. B **53**, 6665 (1996).
[7] T. Lindenau, M. L. Ristig, K. A. Gernoth, J. Dawidowski, and F. J. Bermejo, Int. J. Mod. Phys. B **20**, 5035 (2006); in *Proceedings of the 13th International Conference on Recent Progress in Many-Body Theories*, edited by E. Susana Hernandez and Horacio M. Cataldo, Series on Advances in Quantum Many-Body Theory Vol. 10 (World Scientific, Singapore, 2006), p. 67.
[8] J. Dawidowski, F. J. Bermejo, M. L. Ristig, C. Cabrillo, and S. M. Bennington, Phys. Rev. B **73**, 144203 (2006).
[9] K. A. Gernoth, Ann. Phys. (N.Y.) **285**, 61 (2000); **291**, 202 (2001).
[10] K. A. Gernoth, M. J. Harrison, and M. L. Ristig, Int. J. Mod. Phys. B **20**, 5057 (2006); *Proceedings of the 13th International Conference on Recent Progress in Many-Body Theories*, edited by E. Susana Hernandez and Horacio M. Cataldo, Series on Advances in Quantum Many-Body Theory Vol. 10 (World Scientific, Singapore, 2006), p. 91.
[11] I. Silvera and V. Goldman, J. Chem. Phys. **69**, 4209 (1978).
[12] G. Senger, M. L. Ristig, K. E. Kürten, and C. E. Campbell, Phys. Rev. B **33**, 7562 (1986).
[13] B. A. Younglove, J. Phys. Chem. Ref. Data Suppl. **11**, 1 (1982).
[14] C. E. Campbell, Phys. Lett. **44A**, 471 (1973).
[15] B. E. Clements, E. Krotscheck, J. A. Smith, and C. E. Campbell, Phys. Rev. B **47**, 5239 (1993).
[16] M. Celli, U. Bafile, G. J. Cuello, F. Formisano, R. Magli, E. Guarini, M. Neumann, and M. Zoppi, Phys. Rev. B **71**, 014205 (2005).
[17] L. Verlet, Phys. Rev. **165**, 201 (1968).
[18] R. P. Feynman, Phys. Rev. **94**, 262 (1954).
[19] F. J. Bermejo, B. Fåk, S. M. Bennington, R. Fernandez-Perea, C. Cabrillo, J. Dawidowski, M. T. Fernandez-Diaz, and P. Verkerk, Phys. Rev. B **60**, 15154 (1999).
[20] R. Pantförder, T. Lindenau, and M. L. Ristig, J. Low Temp. Phys. **108**, 245 (1997).
[21] M. Celli, D. Colognesi, and M. Zoppi, Phys. Rev. E **66**, 021202 (2002).
[22] M. Zoppi, D. Colognesi, and M. Celli, Eur. Phys. J. B **23**, 171 (2001).
[23] M. L. Ristig, G. Senger, M. Serhan, and J. W. Clark, Ann. Phys. (N.Y.) **243**, 247 (1995).
[24] M. L. Ristig, T. Lindenau, M. Serhan, and J. W. Clark, J. Low Temp. Phys. **114**, 317 (1999).